2D - 3D HYBRID PEROVSKITES FOR PEROVSKITE SOLAR CELLS

H.K.Y. Pivini Gunasekara

(179433P)

Degree of Master of Science

Department of Material Sciences

University of Moratuwa

Sri Lanka

February 2020

2D - 3D HYBRID PEROVSKITES FOR PEROVSKITE SOLAR CELLS

Heenatigala Kanaththage.Yeshani Pivini Gunasekara

(179433P)

Thesis submitted in partial fulfillment of the requirement for the degree of Master of Science

Department of Material Sciences

University of Moratuwa

Sri Lanka

February 2020

DECLARATION

I declare that this is my own work and this thesis does not incorporate without acknowledgement any material previously submitted for a Degree or Diploma in any other University or institute of higher learning and to the best of my knowledge and belief it does not contain any material previously published or written by another person except where the acknowledgment is made in the text.

Signature: …….. Date: …….....

H.K.Y.P.Gunasekara

The above candidate has carried out research for the Master of Science under my supervision.

Signature of the supervisor: …… Date: ……

Dr. Galhenage A.Sewvandi

ACKNOWLEDGEMENT

It is with great pleasure and a sense of gratitude that I thank my supervisor Dr. Galhenage A.Sewvandi for guiding me, encouraging me to initiate, and see me through the completion of this study.

I especially thank every member Department of the Material Sciences, University of Moratuwa for helping me in one way or the other. I am grateful for Dr.Nuwan de Silva for his support. My thanks are extended to Mr. Mihiranga Jayaweera for the support and providing the facilities to carry out the analysis undertaken for this study. I thank all of the willing hands that helped me in field and laboratory work, especially the technical assistance, their help, concern and the overall atmosphere of friendship, I am thankful to each one of them.

The tremendous contributions made by my parents and my family who guided me this far. Especially I thank Mr. Thejan Rajapakshe for his tremendous support. Finally, this would not have been completed without the love and support of all my friends and associates mentioned and unmentioned. I thank them for their patience and help.

ABSTRACT

Hybrid Organic-Inorganic Perovskites (HOIP) have been studied extensively and grown popular. Especially in Three-dimensional (3D) Perovskites, achieving power conversion efficiency (PCE) exceeds 23%. Nevertheless, some of the morphological imperfections will limit their structural capabilities. Pinholes in discontinuous perovskite films induces the huge leakage current which can cut down the device efficiency and creates a short circuit. Therefore, it is essential to deposit a compact film with passivated defects. Two-dimensional (2D) halide perovskites, conversely attracted significant attention and become a positive alternative with their uncomplicated synthesis, stability, and excellent photoelectric properties. This study, investigates the formation and properties of 2D Tetrabutylammonium lead halide ($TBAPbBr_xI_{3-x}$) HOIP. Tetrabutylammonium ion is a large cation, and more likely forms a 2D perovskite structure which was confirmed by the XRD spectrum. Substantiate by SEM images, $TBAPbBr_xI_{3-x}$ establishing and favors crystals with enhance orientation and few grain boundaries and. However, the absorption spectra of the film shows an excitonic peak at 411 nm and a clear band edge at 450 nm. Resulting in poor absorbance in the visible range, with optical band gap of 2.76 eV, narrowing the ability to use $TBAPbBr_xI_{3-x}$ alone in solar cells. Conversely, $TBAPbBr_xI_{3-x}$ can use as separate capping layer on the top of 3D perovskite layer, enhancing the properties of the 3D perovskite layer. Incorporating $TBAPbBr_xI_{3-x}$ into $CH_3NH_3PbI_3$ shows a better film formation with few holes. The application of mixed perovskite layers incorporated solar cells will result in better structural and optoelectronic properties.

Keywords— Hybrid Organic-Inorganic Perovskites, Two-dimensional, Tetrabutylammonium lead halide, pinholes

TABLE OF CONTENTS

TABLE OF FIGURES

List of Abbreviations

PV: photovoltaic

PCE: power conversion efficiency

HOIPs : Hybrid Organic-Inorganic Perovskites

PSC: perovskite solar cells

DSSC: dye-sensitised solar cell

MA: methylammonium

FA: formamidinium ion

DMF: N,N-dimethylformamide

TBA: Tetrabutylammonium ion

TBABr: Tetrabutylammonium Bromide

PbI_2: lead(II) iodide

$TBAPbBr_xI_{3-x}$: Tetrabutylammonium lead bromide/ iodide

$MAPbI_3$: methylammonium lead iodide

XRD: X-ray diffraction

SEM: Scanning Electron Microscope

t: tolerance factor

μ: octahedral factor

LIST OF APPENDICES

1. INTRODUCTION

Energy demand in the world is increasing significantly with an increase in the population and the advancing economy over the last few years. Photovoltaic (PV) solar cells, being the world's largest green energy source, are capable of transforming the solar energy directly into the electrical energy. The usage of solar energy for electricity generation increases by an average of 8.3% per year [1], to meet the entire world's energy demand. Today around 95% of the installed photovoltaic capacity is supplied by solar cells made from silicon and other reaming created through thin film technologies. The high production cost of crystalline silicon solar cells due to the necessity of extremely high quality raw elements and a high processing temperature has traditionally been used as an argument for the inability of the large scale application of this technology. Moreover, the drawback of these thin film technologies is that they require highly toxic, very costly materials. Hybrid Organic-Inorganic Perovskites (HOIPs), with ABX_3 structure, have been studied extensively for their structural and optoelectronic properties for solar cell fabrications. The solar-cell industry requires high efficiencies, simple processability, low cost, and high accessibility of raw materials for the production. HOIPs enables an enormous number of opportunities to integrate all these requirements due to the additional functionalities and structural flexibilities of organic structures [2].

Kojima and co-workers reported the first solar cell based on perovskite compounds. They achieved the power conversion efficiencies (PCE) of 3.81% using methylammonium lead iodide ($MAPbI_3$) [3]. Three-dimensional (3D) perovskites (mainly methylammonium lead halides, $MAPbX_3$), have achieved power conversion efficiency (PCE) over 23% by 2019 [4]. $MAPbI_3$ being an excellent solar absorber with a high extinction coefficient enables its remarkable photovoltaic performance. Nevertheless, the pinholes in the perovskite film induce a huge leakage current which can reduce the device efficiency by creating a short circuit [5]. Therefore, it is essential to deposit a compact $MAPbI_3$ film with passivated defects. The diverse chemical structure of these organic components facilitates significant openings for the alteration and modification of the structure, a vast number of chemical possibilities to the final

perovskite. To resolve the issues, researches have altered the 3D structure by using ~~a~~ different chemical compounds to both A and X sites, resulting in lower-dimensional layered structures [2, 4, 6]. Lately, improvements in the low-dimensional perovskite materials and find out their properties for the optoelectronic device performances gained the increased attention [7]. Two-dimensional (2D) halide perovskites attracted significant courtesy and have become a positive alternative owing to their uncomplicated synthesis, stability, and excellent optoelectronic properties. Moreover, it can be used as a capping layer, a light absorber, a passivating layer, and/or a mixed 2D/3D perovskite structure [2, 7, 8]. In which researchers have been able to produce 2D/3D perovskite hybrid materials with the stability which lasts for one year. Furthermore, it reaches equivalent performances compared with the 3D perovskite device [9]. There is a need for an optimized production pathway and their behaviour on Organic-inorganic perovskite materials.

In this study, I have investigated the formation and properties of 2D tetrabutylammonium lead halide ($TBAPbBr_xI_{3-x}$) HOIP. Tetrabutylammonium (TBA) ionic additive replaced as the A-site organic cation in the perovskite structure. Moreover, to improve performance in the 3D perovskite structure, $TBAPbBr_xI_{3-x}$ perovskite thin film introduced on the top of the $MAPbI_3$ structure as a capping layer. Which can cover the pinholes and provide the extra moisture-resistant ability by efficient passivation of the defects in the 3D perovskite structure.

2. LITERATURE REVIEW

2.1 Introduction

Global warming is one of the world's major issues, which is caused by the emission of greenhouse gases (mainly CO_2) from burning coal and oil. The world population and the economy have grown exponentially over the last few years. According to the U.S. Energy Information Administration, demand for energy has increased significantly with a projected increase in energy consumption of ~28% from 169 PWh in 2015 to 216 PWh in 2040 [10]. To initiate and implement affordable, clean, and sustainable energy sources to meet today's energy requirements is the biggest challenge. The energy supplied on earth by solar radiation is an efficient and feasible source to harvest and convert into electricity. The usage of solar energy for electricity generation increases by an average of 8.3% per year as a suitable substitute, to meet the entire world's energy demand [1].

2.2 Solar Cells

After the discovery of a naturally formed silicon p-n junction by Russell Ohl and patented in 1941, and the improvement of the production process, Chapin, Fuller, and Pearson developed the first "modern" silicon solar cell. It converted 6% of the incident sunlight energy into electrical energy [11]. The operation of a solar cell depends on the absorption of light, the successive charge generation, transportation, and assembly. The semiconductor material is used to form the active layer of the solar cell. Semiconductor materials are characterized with a bandgap, which is the energy gap that separates, the band occupied with electrons (the valence band, VB) from that of with empty states occupied (the conduction band, CB). The magnitude of the bandgap defines which photons are able to be absorbed by the material. From the VB to the CB electron is excited, when the incoming photon energy is larger than, or equal to the bandgap. In most inorganic semiconductors, the electron and hole can be considered as free charges at room temperature. When the electron and hole are strongly bound through Coulomb interaction, due to a low permittivity as commonly found in organic semiconductors, the electron-hole pair is referred to as an exciton. The exciton must be separated into one negatively charged electron and one positively charged hole that

can move spontaneously through the material for a photovoltaic effect. After generation and separation, the electrons are collected through an electrode into an external circuit, where they dissipate energy and produce power before returning to the solar cell at the opposite electrode, where it recombines with the hole, closing the charge cycle.

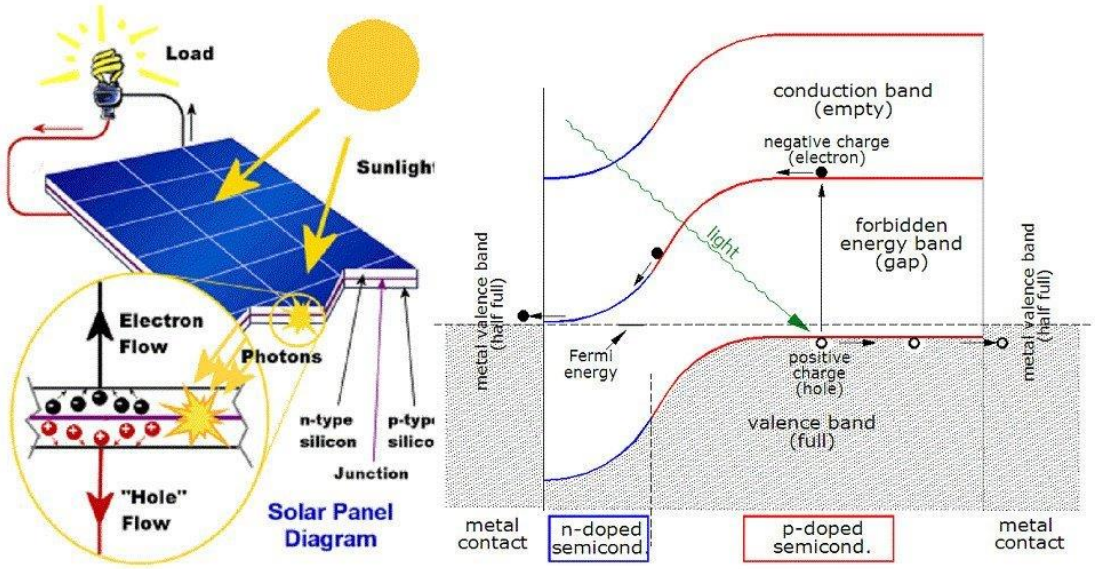

Figure 1- Illustration of solar cell theory [12]

Today, almost 95% of the installed photovoltaic (PV) capacity is supplied through solar cells made from silicon and other remaining structures created by thin film technologies. Silicon solar cells have been studied extensively over the past few decades, achieving high power conversion efficiencies (PCE) reached 29% in a single junction structure [13]. This is already approaching the theoretical thermodynamic power conversion efficiency limit in the sunlight calculated by Shockley and Queisser in 1961. Theoretically, PCE as high as 33.7% for a single p-n junction solar cell with a 1.4 eV bandgap [14].

Crystalline silicon solar cells are completely governing the profitable and photovoltaic (PV) markets, although they are not cost effective. The necessity of extreme purity of raw materials and processing at the high temperature of crystalline silicon solar cells results in high manufacturing cost.

The high production cost of silicon solar cells has traditionally been used as an argument for the economic viability of the large scale application of this technology. However, the upscaling of silicon solar panel production and maturing of technology have drastically reduced the production costs in recent years, making it a much more competitive technology [15]. The fact that crystalline silicon is an indirect bandgap material, however, requires the semiconductor layer to be relatively thick (~200 μm), and the construction of the panels become comparably substantial and making flexible PV applications nearly impossible. Thin film photovoltaics aim to reduce the weight and material cost by applying a thin active layer (< 5 μm), which is made possible by the use of a direct bandgap semiconductor absorber. solar cells using amorphous silicon (a-Si), cadmium telluride (CdTe), copper indium gallium selenide (CIGS) and gallium arsenide (GaAs) thin film, have reached efficiencies of up to 14.0%, 22.1%, 22.6%, and 28.8% respectively (Figure 2) are the most popular and leading technologies in solar cell industry [16].

However, the major drawback of these thin film technologies, are the highest efficiency devices requiring the use of highly toxic, very costly materials and difficult production methods are difficult. Recently, as a new thin film PV technology, metal halide perovskites emerged. Perovskite solar cells show promising initial results and an impressive increase in PCE in a few years.

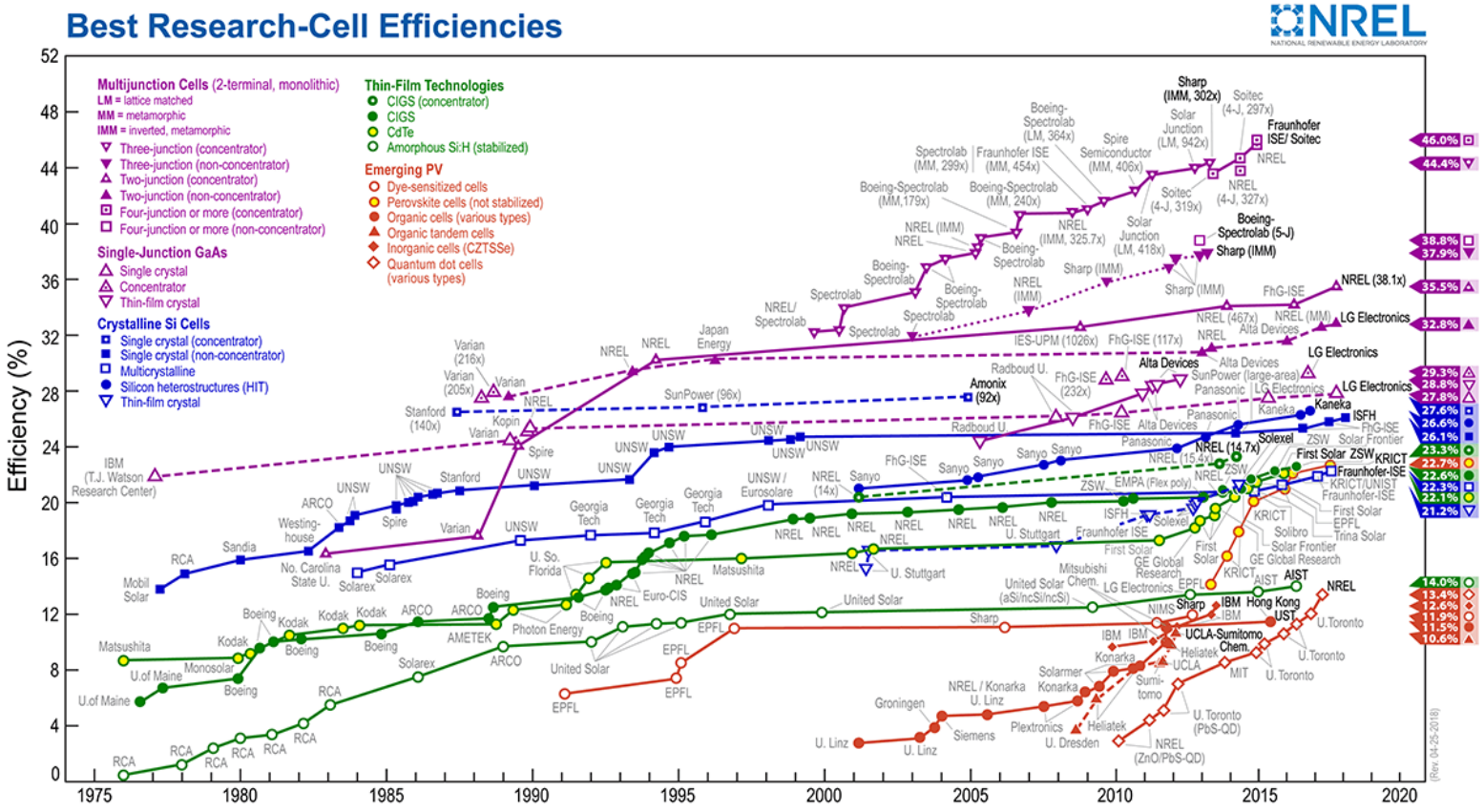

Figure 2- Efficiency Chart by National Renewable Energy Laboratory, NREL efficiency chart, https://www.nrel.gov/pv/assets/images/efficiency-chart.png.

2.3 Perovskite Structured Materials

The mineral $CaTiO_3$ was discovered by Geologist Gustav Rose in the Ural Mountains in 1839. It was named perovskite in gratitude to Count Lev Alexevich von Perovski, a renowned Russian mineralogist [17]. The Earth's crust covers numerous types of perovskites. Among them $MgSiO_3$ and $FeSiO_3$ are abundant. The perovskite family consists of numerous types of chemical formule including transition metal oxides with the formula ABO_3 [18]. The name perovskite refers to any member of a very large family of compounds that has a definite crystal structure with the ABX_3 formulation with a larger A cation, smaller B cation, X anions (X = oxygen, halogen). The A cation occupies a cubo octahedral site shared with twelve X. The B cation is stabilized with an octahedral site shared with six X [19].

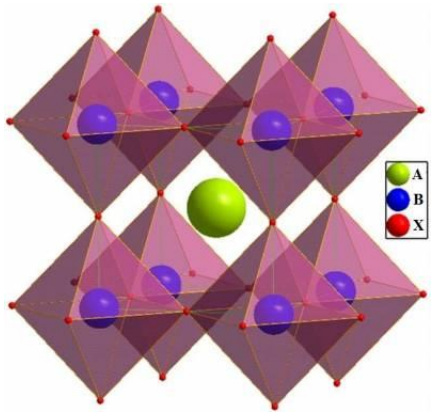

Figure 3- Perovskite Structure (https://www.ucl.ac.uk/institute-for-materials-discovery/research/clean-energy/perovskite-solar-cells)

Crystal structures of perovskite and perovskite-related halides make themselves valuable by possessing properties such as electron-acceptor behaviour; a large optical transmission domain; high resistivity; antiferromagnetic; exceptional magnetic; piezoelectric; photoluminescent properties; anionic conductivity over a wide temperature range and many more [20]. Furthermore, it is one of the structures that are most repeatedly encountered in solid-state physics accommodating a large number of metal ions in the periodic table.

2.4 Hybrid Organic–Inorganic Perovskites

Hybrid organic–inorganic perovskites (HOIPs) which have the structure of ABX_3 materials in which the A-site replaced by organic amine cations and/or X-site ions are substituted by organic linkers. The Solar cell industry requires high PCE, simple processability, low cost, and high accessibility of raw materials for production. HOIPs enables an enormous amount of opportunities to integrate all these requirements [2, 20]. Especially, additional functionalities and structural flexibility are aided by organic constituents in the structure of these HOIPs. Most significantly, the diverse chemical structure of these organic components facilitate significant openings for alteration and modifying the structure, a vast number of chemical possibilities to the final perovskite [22].

Kojima and co-workers reported the first liquid state solar cells based on perovskite compounds. They achieved the PCE of 3.81% using $CH_3NH_3PbI_3$ to construct the photovoltaic cell [3]. The current recorded for perovskite solar cell PCE, stated by the Chinese Academy of Sciences in 2018 was 23.7% [4]. It was certified by the National Renewable Energy Laboratory in the United States [4, 22].

Differences in organic components and metal salts, facilitates a large number of chemical possibilities, covering a significant part of the periodic table for the formation of HOIPs. With the enormous possibilities, it is essential to model the formation of stable perovskite. One of the parameters which predict the stability is the Goldschmidt tolerance factor (t), by which the ratio of ionic sizes that perovskite structure can endure is specified. This is a semi-empirical approach for evaluating size which can withstand in the structure. It can monitor the design and synthesis pathway for promising HOIPs with preferred modifications. To form a stable 3D cubic perovskite structure, size of the ions should meet the ionic radius (r) of A, B and X must satisfy the tolerance factor to be within the range of $0.81 < t < 1.11$ [7, 23] ;

$$t = \frac{rA + rX}{\sqrt{2}(rB + rX)} \tag{1}$$

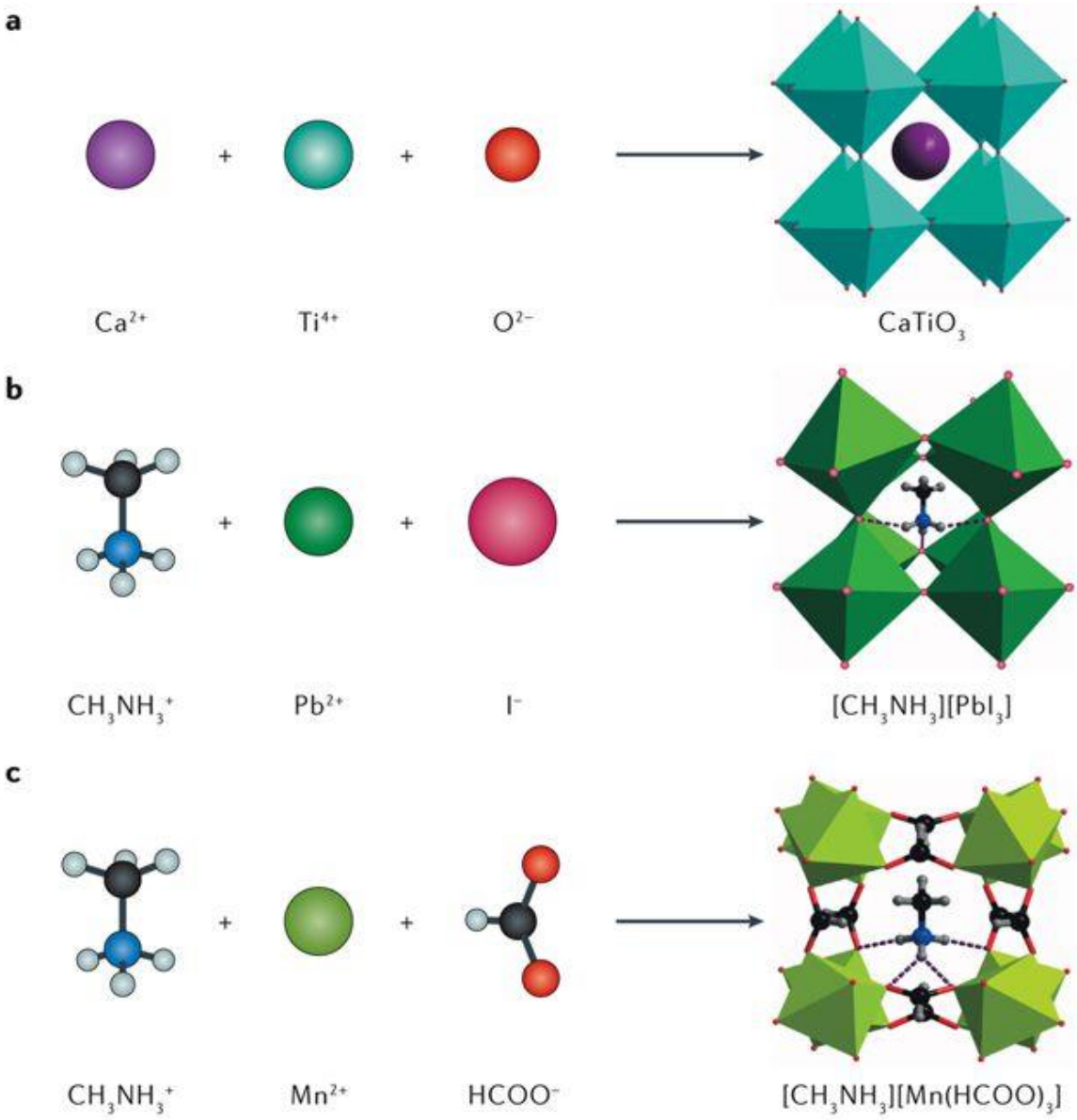

Figure 4 - ***The evolution of perovskites*** *[7]****.*** *The evolution from perovskite oxides to hybrid organic–inorganic perovskites (HOIPs) with an organic A-site, then to HOIPs with both organic A- and X-sites. (a). Inorganic perovskite oxide (b). HOIP with an organic cation at the A-site, (c). Example of a HOIP with an organic cation at the A-site and an organic anion at the X-site (a metal–organic framework perovskite)*

This simple semi-empirical method for evaluating size compatibility can direct the rational structures and synthesis of new HOIPs using arrangements with desired functionalities. Nonetheless, the tolerance factor shows restricted appropriateness to

formulating the stability of HOIPs. Furthermore, the octahedral factor (μ), a geometric aspect was proposed which should be in $0.44 < \mu < 0.9$.

$$\mu = \frac{rB}{rX} \tag{2}$$

This can be used to evaluate the affinity of the A and B-site cations. Further, it defines the fit of the B-site cation into the X_6 octahedron on the perovskite structure.

2.5 Morphological Properties of HOIPs

In organic and inorganic materials, crystallinity plays a vital role in defining electronic properties [25]. Perovskite semiconductors are a class of polycrystalline materials. Polycrystalline materials synthesized using lower-temperature methods are made up of grains separated by grain boundaries. In determining the optoelectronic properties of a semiconductor grain boundaries play an important role. Generally, grain boundaries act detrimentally for device performances [26]. Theoretically, it can perform as non-radiative recombination centers, and afterward impairs the optoelectronic properties of perovskite structures [27]. Grain boundaries are the cause for flaccid bonds, vacancies, and other imperfections. For the best performance, high-performing semiconductor devices are needed, which require high quality and defect free materials [26]. Several groups including Chu and co-workers, Xiao and co-workers, and De Marco and co-workers mentioned that the device performance is often expressively enhanced composed with elongated charge-carrier lifetimes when the grain size is enlarged from a few hundred nanometres to the micrometer level [24, 27, 28]. Liu and co-workers found that by altering the organic cation, the grain arrangement of the perovskite can be controlled [30]. Cao and coworkers suggested, that flawless thin films can be achieved with 2D perovskites [6]. Oriented crystals with limited grain boundaries are establishing in structures because of the 2D arrangement of compounds, [6].

Additionally, the methodology and the solvents those have been used to synthesize the perovskite film will greatly affect the grain structure(Figure 5) [1,25].

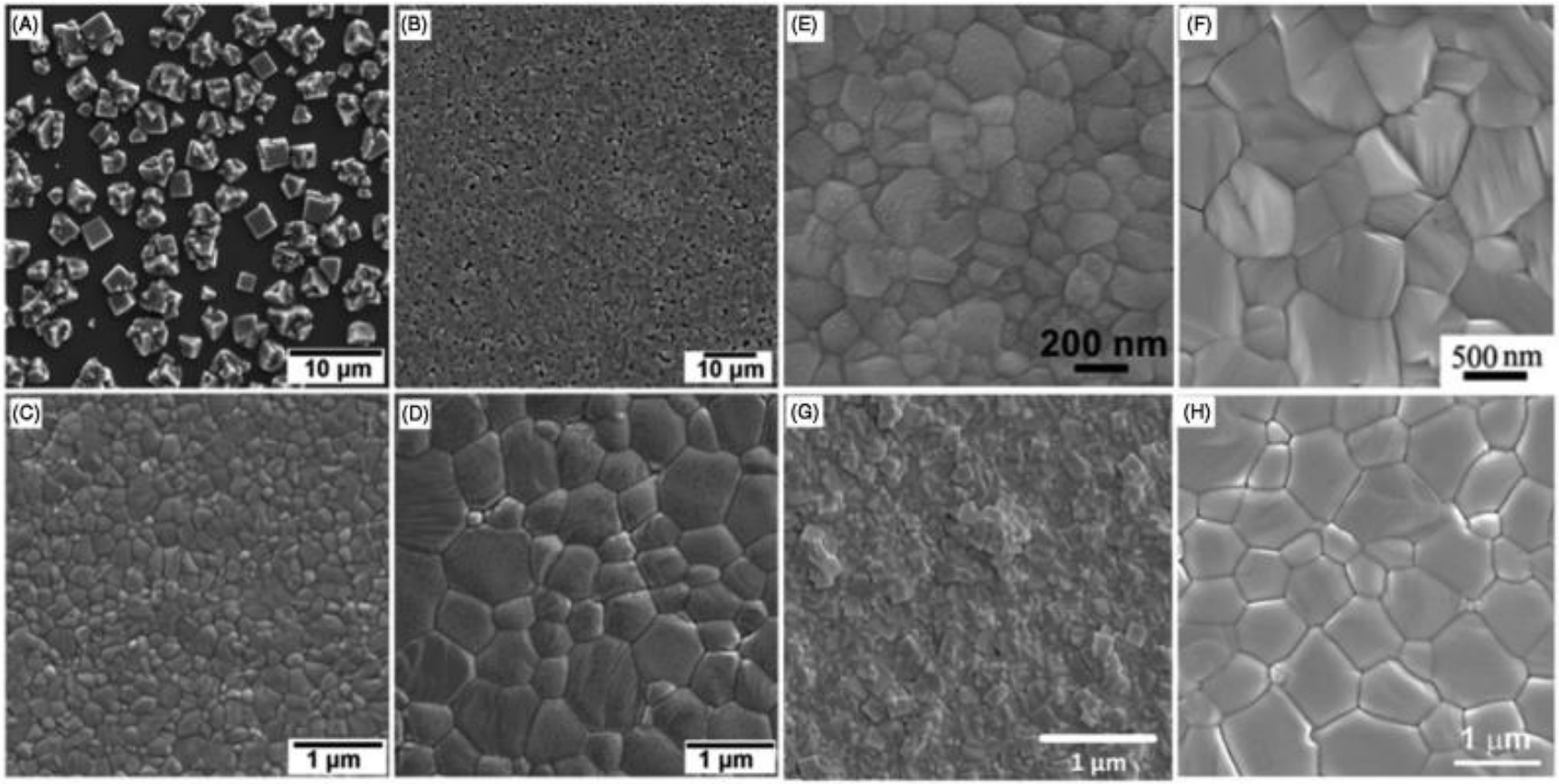

Figure 5 - Morphology control of hybrid organic–inorganic metal halide perovskite films: SEM images of $MAPbI_3$. (A) one-step spin coating, (B) two-steps spin coating, (C) one-step spin coating with toluene treatment, (D) thermal annealing of toluene treated film, (E) solvent–solvent extraction method, (F) vapour assisted deposition method, (G) vapour deposition method, (H) fast deposition crystallization method [1].

2.6 Optical Properties of HOIPs

In terms of materials and properties, best performing PV applications require an appropriate band gap that matches the solar spectrum [32]. The exciton, characteristically procedures in its structure when a photovoltaic cell absorbs incident light. The exciton consists of an electron that has pushed into the CB by a received photon and the positively charged hole in VB.

An organic cation can be replaced with an inorganic cation, which introduces an opportunity for tuning the chemical bonding and optical response [33]. The band structure can be calculated with the many-body perturbation theory in the GW approximation including spin-orbit coupling, which the approach for obtaining band structures theoretically. Theoretically, it gives ~1.7 eV fundamental bandgap for $MAPbI_3$. Experimentally, an optical band gap of ~1.6 eV when optical absorption at room temperature [2]. Furthermore, when methylammonium is replaced with the formamidinium ion (FA) forming formamidinium lead halide this has a bandgap of 1.48 eV [1]. It is therefore evident that changes in organic cation can change the light absorption properties and bandgap of perovskites.

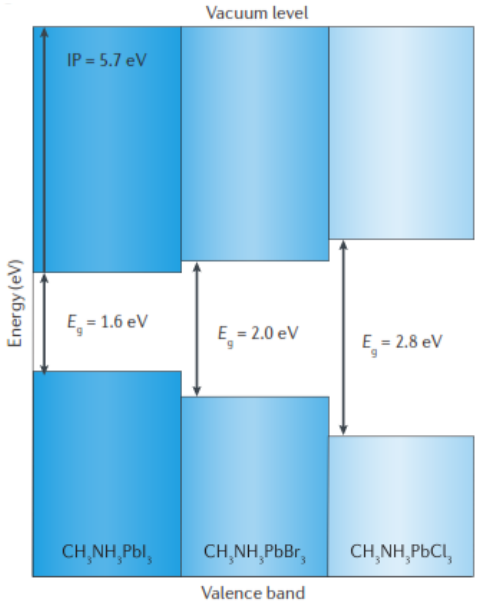

Figure 6 - Fundamental bandgaps of different hybrid organic–inorganic perovskites (HOIPs) calculated in the GW approximation, demonstrating that the bandgap can be tuned by the halide atom [2]

Moreover, chemical modification can be done to the anions in the structures of HOIPs (Figure 6) [1]. It facilitates tuning the bandgap over a broad range of the solar spectrum. Bhandari and Ellingson stated that when you introduce Br ion into the perovskite structure, it can be adjusted to cover nearly the whole visible range of the solar spectrum. It has the bandgap of 1.5 eV for $MAPbI_3$ to 2.3 eV for $MAPb(Br_xI_{1-x})_3$ [1].

2.7 Advantages and Challenges in HOIPs

Beyond doubt, in solar cells, perovskite materials are suitable for use as an active material. The high absorption coefficient, low exciton binding energy, and efficient ambipolar charge transport capabilities of the material make the production of highly efficient thin film devices possible. Due to the high solubility of precursor materials, low cost solution processing of the perovskite layer is an attractive option. Even though the record PCE of perovskite solar cells is approaching that of the industry giant silicon, the price of silicon solar panels has dropped so significantly due to the development and maturing of the fabrication processes, resulting the low material costs of perovskite solar cells is no longer a strong selling point for the technology. The high tolerance for defects and the ability to change the composition of the material towards specific applications for HOIPs are the unique advantages of perovskite materials. Combining these with a large number of diverse processing methods that have been developed, the way is paved in the application of perovskite solar cells in large area applications as well as niche markets, for example, flexible and tandem solar cells.

The main challenge for the perseverance of the perovskite solar cell technology is the toxicity of the lead that is used in the HOIPs like in $MAPbI_3$. It will hinder the speed of commercialization. However, calculations and studies have shown that the amount of lead in perovskite solar panels is far from catastrophic for the environment or the public. Recycling is seemed a viable option. Additionally, alternatives such as tin (Sn) might be more toxic to the aquatic environment than lead [34].

Furthermore, the long term stability of the material under operating conditions still deserves attention. Stability is probably the biggest challenge preventing practical applications of perovskite solar cells. Especially due to the polycrystalline nature and

poor thermal stability perovskites are is decomposed at a temperature above 100 °C, degradation in the presence of moisture, and a huge number of morphological and energetic imperfections are existing in perovskite films. In $MAPbX_3$ the device performance is reduced by the radiative recombination. One of the major problems is that it is not photo-stable (under different illumination and biasing conditions, the device performance fluctuates). Moreover, the pinholes in the discontinuous perovskite film induced the huge leakage current which can cut down device productivity and even producing a short circuit [35]. Therefore, it is essential to deposit a compact $MAPbX_3$ film with passivated defects.

Thus, improved architecture and proper encapsulation methods are necessary for the durable and stabilized perovskite solar cell (PSC) production.

2.8 Strategical Approaches to Overcome the Challenges

Approaches have been made to reduce moisture absorption and to enhance the efficiency of PSC in the past few years. Encapsulation, coating layers, surface modification (incorporate additives), and 2D/3D perovskites fabrication are the major strategies that have been undertaken to overcome the above problems. Encapsulation is a protection method to make the cell chemically stable by the selection of sealing materials with high temperature performance [34]. However, it leads to significantly higher manufacturing costs making it an unfavourable method for commercial production [36]. Subsequently, as a novel coating layer to the perovskite structure, high-cost hole transport material, organic HTM spiro-OMeTAD ($C_{81}H_{68}N_4O_8$) was introduced in 2014. It was substituted with polymethylmethacrylate (PMMA) which is a conducting carbon nanotube–complex. This new layer was primarily introduced to the cell to mitigate thermal degradation [37]. Lately, fluorinated photo-polymer coatings and hydrophobic polymers were introduced and placed on top of the perovskite structure establishing a strong hydrophobic barrier.

Introducing small molecules such as alkyl ammonium cations to increase moisture stability is the third approach. These molecules can adsorb into the surface of the perovskite layer to ameliorate the humidity tolerance and passivating exterior defects. Alkyl ammonium cations be able to be used, where the perovskites layer immersed

into alkyl ammonium solutions [38]. The application of these interlayers can hinder perovskite degradation. The additive strategy is one of the approaches that has been used as an effective means to overcome the induced leakage current through pinholes in the intermittent perovskite layer. Besides, it prevents complex device fabrication operations. Both anions and cations containing in the ionic additives could occupy the openings in the perovskites layer, as well as it can affect the crystal arrangement of perovskite grains.

The final approach is the formulating of 2D/3D perovskite hybrids which is a very encouraging method. In this approach, researchers have been able to produce perovskite solar cells with stability lasting for one year. Furthermore, it reaches equivalent performances compared with the 3D perovskite device [8].

2.9 Tetrabutylammonium Bromide

Tetrabutylammonium bromide (TBABr) is an ionic additive. Tetrabutylammonium (4(C4H9)N+, TBA) is one of the alkylammonium cations. Tetraalkylammonium cation has been comprehensively used for its amphiphilic (having both hydrophilic and hydrophobic parts) ability in the crystallisation and templating zeolites and additional absorbent constituents [39]. The pre-formed perovskite films are immersed in a solvent contains TBA and the alkylammonium cations are collected on the upper layer of the perovskite structures to functionalize the exterior. Ammonium cations are effortlessly adsorbed by chemical interactions onto the numerous crystalline surfaces, consequently, onto the perovskite polycrystalline surface, these ammonium cations can be chemically adsorbed by interactions such as ionic or hydrogen bonding. To achieved enhanced coverage and reduced the pinhole size, tetrabutylammonium ions were added into the precursor solution when perovskite structures were synthesized [35].

2.10 Tetrabutylammonium lead halide perovskite

Tetrabutylammonium (TBA), a comparatively large alkyl ammonium cation used as an ionic additive and/or stabilizer in 3D perovskite materials resulting in improved PCE and stability [2, 10]. However, as a capping layer on top of the 3D perovskite

structure using TBA is barely explored. In this study, investigates the formation and properties of 2D Tetrabutylammonium lead halide ($TBAPbX_3$) HOIP, introducing the TBA, as the A-site cation in the perovskite architecture. Then, $TBAPbX_3$ perovskite thin film is introduced as a separate, capping layer on top of the 3D $MAPbI_3$ perovskite structure. 2D $TBAPbX_3$ perovskite layer covers the pinholes and provides extra moisture resistant ability to the structure by efficient passivation of defects in the 3D perovskite structure. Moreover, this layered combination results in similar optical properties to the final perovskite structure comparing with the 3D MAPbI3, enabling efficient use in solar cells.

3. METHODOLOGY

The perovskite, $TBAPbBr_xI_{3-x}$ precursor solution was prepared by dissolving tetrabutylammonium bromide (TBABr) 0.8 mmol (322.37 $gmol^{-1}$, 0.257g, from extra pure AR 99+%, purchased Sisco Research Laboratories Pvt.Ltd SRL) and PbI_2 0.8 mmol (461.01 $gmol^{-1}$, 0.369g, from extra pure AR 99%, Sisco Research Laboratories Pvt.Ltd SRL) in N, N-Dimethylformamide (DMF C_3H_7NO, 99.5%, purchased from Sisco Research Laboratories Pvt.Ltd) to get 35w% solution. The solution was stirred continuously for 2 hours at 60 °C. To prepare $MAPbI_3$, above method was followed using methylammonium iodide 0.8 mmol (158.97 $gmol^{-1}$, 0.127g extra pure AR 98%, purchased from Sigma-Aldrich) and PbI_2 0.8 mmol (461.01 $gmol^{-1}$, 0.369g) in DMF.

After the preparation of the $TBAPbBr_xI_{3-x}$ precursor solution, a sample was obtained for powder XRD analysis by evaporating DMF at 80°C. Following the same procedure for synthesizing precursor solution using DMF, the second sample was spun coated (1000 rpm) on to the glass slide. The third sample was prepared using solution casting on to the glass slide. Films were heated at 80 °C until DMF is evaporated. Films were then used for XRD and SEM analysis.

Perovskite films were also prepared by introducing $TBAPbBr_xI_{3-x}$ as a separate layer on top of the $MAPbI_3$ (Figure 7). First $MAPbI_3$ was spun coated (1000 rpm) into the glass slide. After evaporation of DMF at 80 °C, the $TBAPbBr_xI_{3-x}$ precursor solution was spun coated (1000 rpm) into the same glass slide as a separate layer on top of the $MAPbI_3$. $TBAPbBr_xI_{3-x}$ was deposited as 5% and 10% separate layer on top of the $MAPbI_3$. Then the film was analyzed using XRD and SEM.

The light absorption of the $MAPbI_3$ with the capping layer of 5% $TBAPbBr_xI_{3-x}$, neat $TBAPbBr_xI_{3-x,}$ and neat $MAPbI_3$ films were analyzed using UV-vis Spectrophotometer.

XRD diffraction patterns were taken using a Bruker Advance D8 X-ray diffractometer with a Cu Kα source. Measurements were collected from 2θ values from 5 ° to 80 °. Scanning Electron Microscope (SEM) images were taken on a Carl ZEISS EVO 18 Research SEM, at a voltage of 10 kV. Thin film reflectance measurements were taken using Shimadzu UV-3600 UV/Vis Spectrophotometer, in the range of 800 nm to

350nm. Absorption was calculated using the Kubelka-Munk function. The Kubelka-Munk functions is given by:

$$F(R) = \frac{(1-R)^2}{2R} = \frac{k}{s} = \frac{Ac}{s} \quad (3)$$

Where, R = reflectance; k = absorption coefficient; s = scattering coefficient; c = concentration of the absorbing species; A = absorbance.

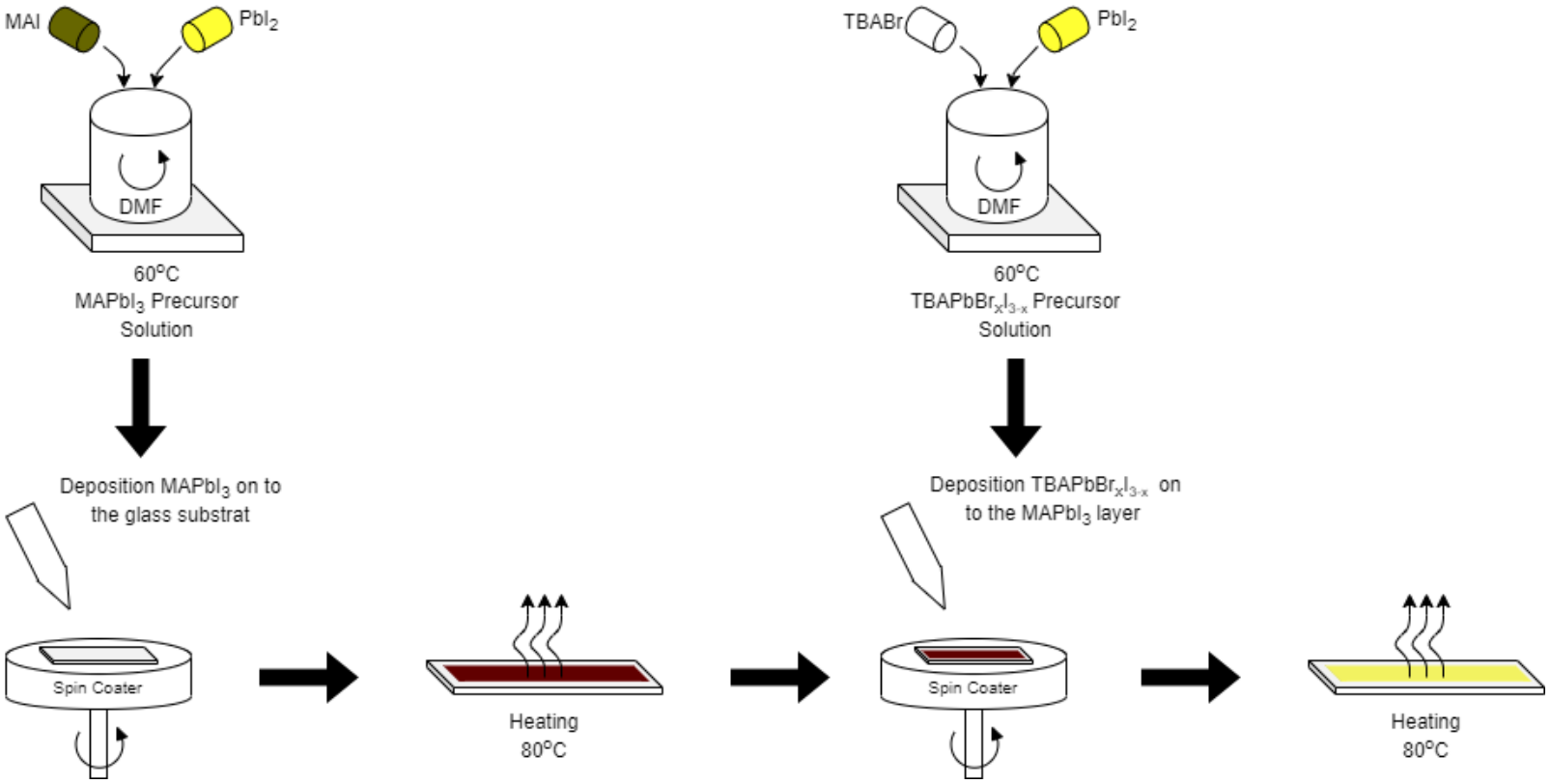

Figure 7 - Methodology of the experiment of the Perovskite films prepared by TBAPbBrxI3-x introduced as a separate layer on top of the $MAPbI_3$

4. RESULTS AND DISCUSSION

4.1 Structural Properties

To form a stable 3D perovskite structure, the size of the ions should maintain the Goldschmidt tolerance factor, t, $0.81 < t < 1.11$ [24]. The ionic radius of TBA is 4.94 Å, which results in a tolerance factor greater than 1.11. It prevents the formation of a 3D structure. As TBA is a large ion, it has a high potential to assemble into a two-dimensional perovskite [36].

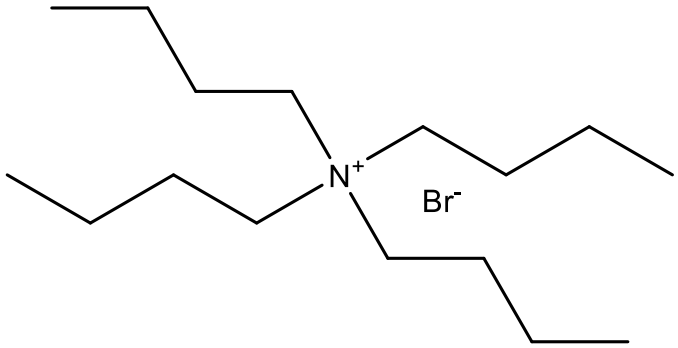

Figure 8- Structure of TBABr

The XRD spectrum (Figure 9. a) confirms the formation of 2D $TBAPbBr_xI_{3-x.}$ Grancini and co-workers mentioned that 2D perovskite materials have consistent peaks at lower angles ($2\theta < 10°$) [8]. Moreover, Yao et al. and Ma et al. point out in both their works, that low angle diffraction peaks detected with mixed 2D/3D HOIPs structures [39, 40]. In this study $TBAPbBr_xI_{3-x}$ perovskite XRD spectrum has a distinguishable diffraction peak at 7.59° which is a characteristic peak that determines the formation 2D perovskite structure. There is no visible peak for unconverted PbI_2 in $TBAPbBr_xI_{3-x}$ It can be considered that a strong interaction has been formed to create a 2D perovskite structure in DMF solution (Figure 9. a).

The XRD spectrum of Figure 9. b shows a sharp and strong peak at 14° (110) and 28° (220) which attributed to 3D $MAPbI_3$ Perovskite structure and confirms the formation of $MAPbI_3$. When the $TBAPbBr_xI_{3-x}$ introduced as a separate layer on top of the

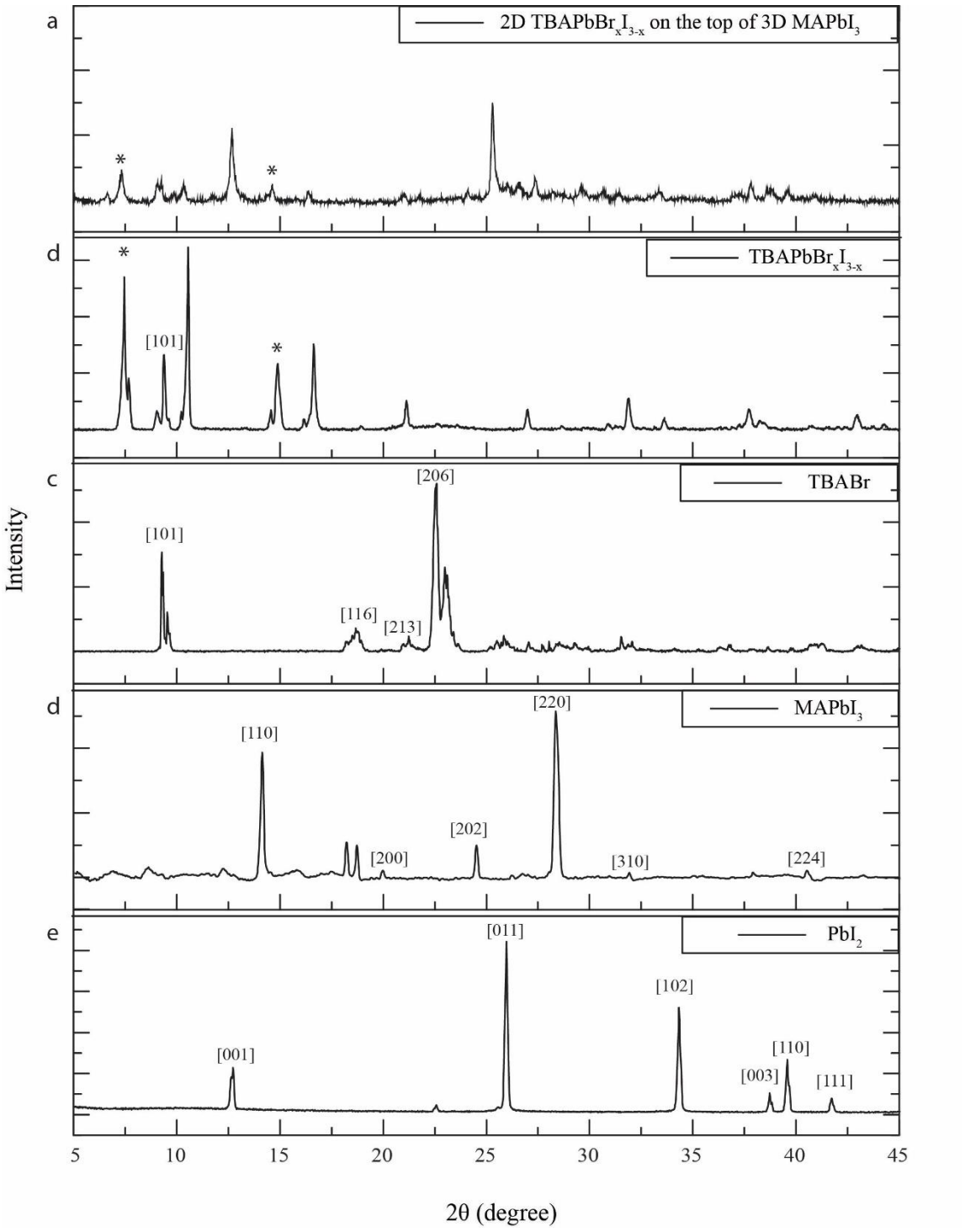

Figure 9 - XRD spectrum of a. $TBAPbBr_xI_{3-x}$ introduced as a separate layer on top of the $MAPbI_3$, b. $TBAPbBr_xI_{3-x}$, c.TBABr, d. $MAPbI_3$, d. PbI_2.

$MAPbI_3$ (1:1), a diffraction peak was observed at 14.6° (Figure 9. c). It correlates with the diffraction peak, at 14.7° in the 2D/3D $(TBA)_n(MA)_{1-n}PbX_3$ structure formed by Poli and coworkers, and it was attributed to TBA [36]. Furthermore, using a solution of cyclopropylammonium iodide (CAI), as 2D perovskite capping layer Ma et al. reported, when the concentration of CAI elevated the strength in the diffraction peak [41] . Poli et al. mentioned that the strength of the peaks of the 3D components is inversely proportional to the concentration of 2D perovskite in the solution [36]. Similarly, in this study intensity of the peaks assigned to 2D $TBAPbBr_xI_{3-x}$ abundant, while the peaks assigned to the 3D $MAPbI_3$ have been reduced (Figure 9.c) when the $TBAPbBr_xI_{3-x}$: $MAPbI_3$ is 1:1.

4.2 Morphological Properties.

Grain structure plays a vital role in device properties. Altering the organic cation, grain structure can be controlled [30]. Quarti et al. stated that the optoelectronic properties can be altered by organic structures in the perovskite [42]. Cao and coworkers suggested, that flawless thin films can be achieved with 2D perovskite [6]. Because of the 2D arrangement of compounds, oriented crystals with limited grain boundaries are establishing in the structures [6]. Considering these facts and SEM images (Figure 11. a), the formation of the 2D perovskite structure is confirmed. The deposition results in yellow, greatly transparent $TBAPbBr_xI_{3-x}$ 2D structure [36].

In addition, 3D perovskite has high moisture instability. As an instance, a film of $MAPbI_3$ will decompose progressively into PbI after a short period of time under normal atmospheric conditions [8]. TBA is a large cation which forms highly oriented and dense perovskite films. Therefore, the moisture stability of these 2D perovskites will enhance by the hydrophobic properties of TBA [8]. SEM images Fig. (11. b, c, d, e, f, and g) was taken to get an understanding of how the TBA enhances the surface properties of the 3D perovskite structure. Fig 11. b, d, and e show large pinholes on $MAPbI_3$ perovskite structure. Fig. 11. c, f, and g show the effect after the addition of $TBAPbBr_xI_{3-x}$ on the top of the 3D $MAPbI_3$ perovskite structure. They show a homogeneous structure with ameliorate surface coverage and few holes. Moreover, coverage improvement is ameliorated when the concentration is increasing (Figure 11.

f and g). Therefore, improved efficiency can be expected by introducing this 2D layer as a capping layer on the 3D structure.

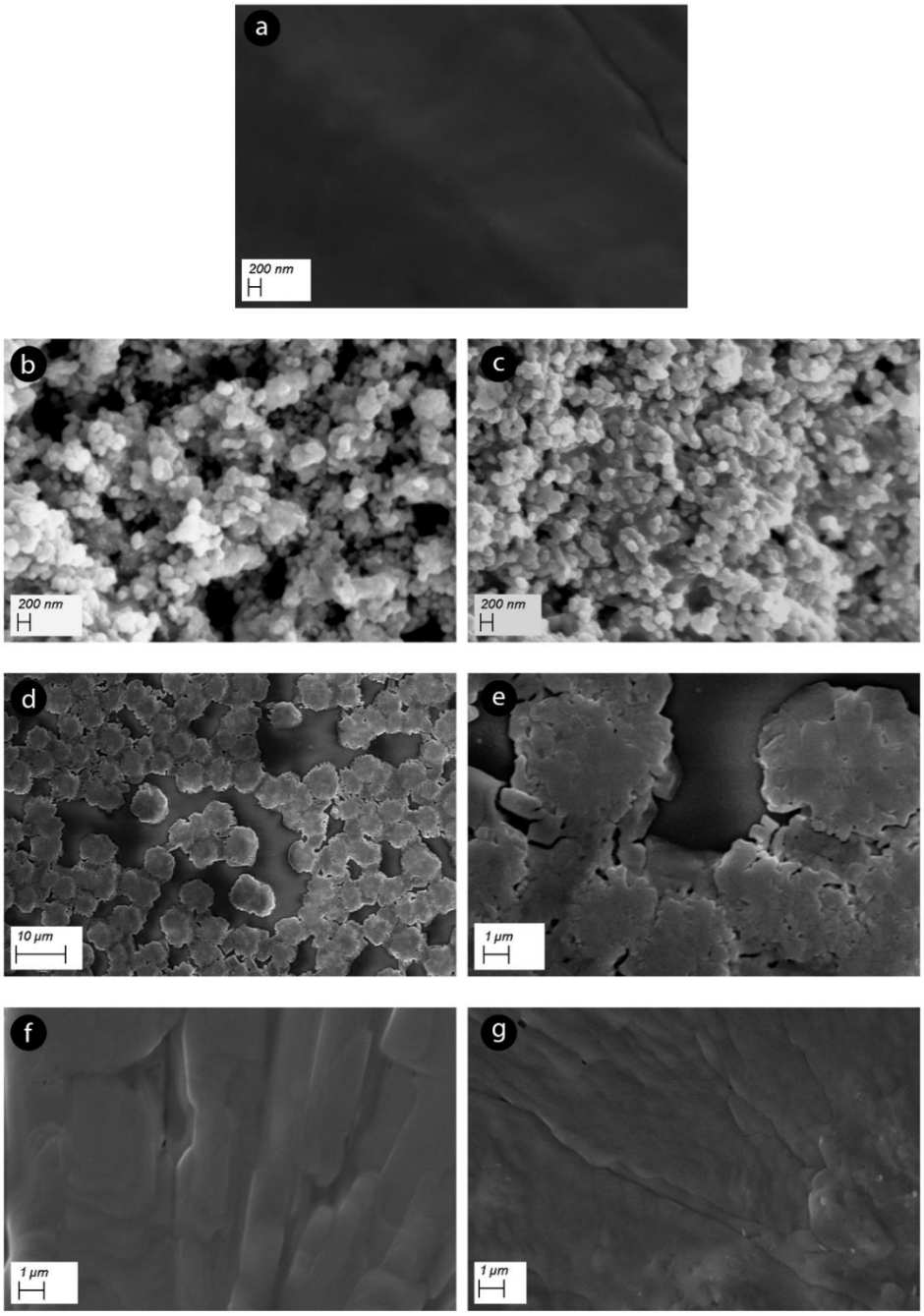

Figure 10- ***a*** *- neat - TBAPbBr$_x$I$_{3-x}$ film,* ***b*** *- solution cast film of MAPbI$_3$,* ***c*** *- solution cast film of TBAPbBr$_x$I$_{3-x}$ on the top of MAPbI$_{3\ (1:1)}$,* ***d*** *and* ***e*** *- spin coated MAPbI$_3$,* ***f*** *- spin coated film of 5% TBAPbBr$_x$I$_{3-x}$ was deposited as a separate layer on top of the MAPbI$_3$,* ***g*** *- spin coated film of 10% TBAPbBr$_x$I$_{3-x}$ was deposited as a separate layer on top of the MAPbI$_3$.*

Despite the fabrication method, the same XRD spectra have been observed. However, the fabrication method clearly affects the grain structure as shown in SEM images (Figure 11). Therefore, altering the fabrication method, better results can be achieved.

4.3 Optical Properties

Figure.12 shows the absorption spectrum of $TBAPbBr_xI_{3-x}$, $MAPbI_3$, and influence after the addition of $TBAPbBr_xI_{3-x}$ as the capping layer on the 3D $MAPbI_3$ perovskite structure. The absorption spectra of the film $TBAPbBr_xI_{3-x}$ shows a distingusable band edge at 450 nm with an excitonic peak at 411 nm. It shows a similar pattern with reported absorption data for 2D perovskites [8]. $TBAPbBr_xI_{3-x}$ reveals poor absorption in the visible range, narrowing the ability to use $TBAPbBr_xI_{3-x}$ alone in the solar cell. Absorption spectra after the addition of 5% $TBAPbBr_xI_{3-x}$ on the top of 3D $MAPbI_3$ perovskite structure indicate a better absorption in the visible range. The application of mixed perovskite layers (2D layer on the top of the 3D layer) incorporated solar cells will results ~~in~~ better structural and optoelectronic properties.

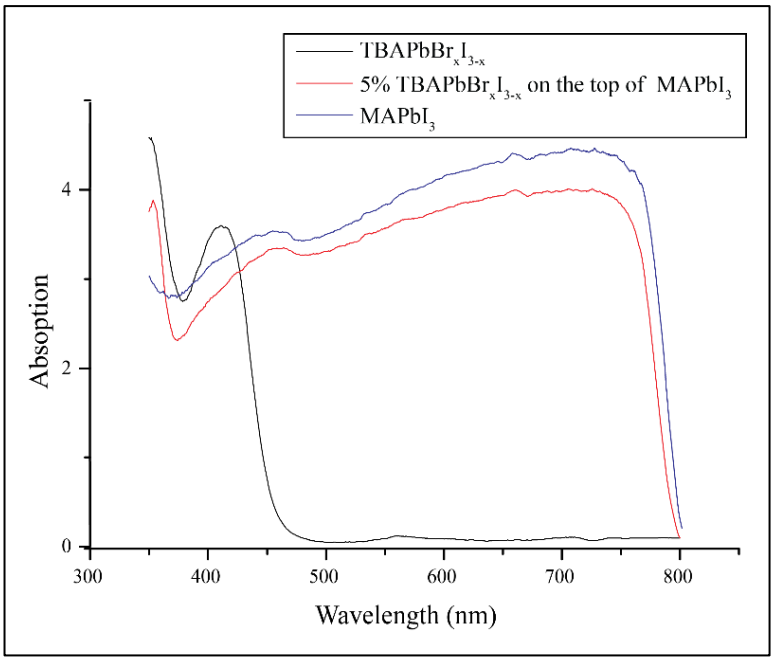

Figure 11 - Absorption spectra of neat $MAPbI_3$, $TBAPbBr_xI_{3-x}$ film and 5% $TBAPbBrxI3_{-x}$ on the top of $MAPbI_3$

A Tauc plot is used to define the optical bandgap of these perovskite materials in Figure 13. The bandgap was calculated from $(\alpha h\nu)^2$ vs hν curve by drawing an extrapolation of the data point to the photon energy axis where;

$$(\alpha h\nu)^2 = 0 \; or \; (\alpha h\nu)^{1/2} = 0 \tag{3}$$

Gives the optical bandgap Eg. Absorption coefficient (α) was calculated using absorbance data,

$$\alpha = 2.303A/t \tag{4}$$

Where t is the thickness and A is the absorbance. Then by the following equation, calculate the bandgap of the semiconductor samples as:

$$\alpha h\nu = A(h\nu - E)^n \tag{5}$$

Where A is a constant, 'h' is the photon energy and 'Eg' is the optical bandgap of the semiconductor, and 'n' is an index related to the density of states for the energy band. It is assumed, n = ½ for direct allowed and n = 2 indirect allowed transitions, respectively.

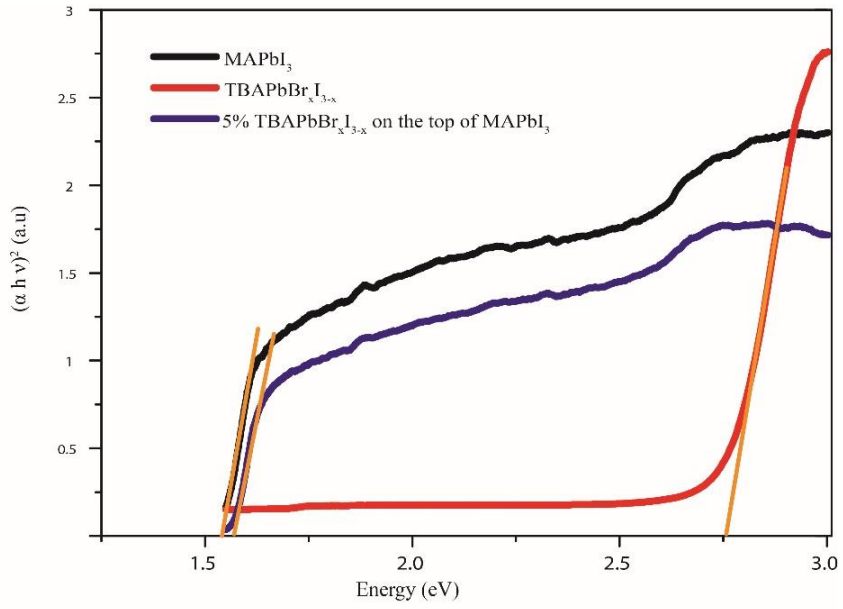

Figure 12- Optical Bandgap of $MAPbI_3$, $TBAPbBr_xI_{3-x}$ film and 5% $TBAPbBr_xI_{3-x}$ on the top of $MAPbI_3$

For neat TBAPbBr$_x$I$_{3-x}$ optical bandgap is 2.76 eV. The TBAPbBr$_x$I$_{3-x}$ on the top of the 3D MAPbI$_3$ perovskite structure has a bandgap of 1.56 eV. It was very close to the neat MAPbI$_3$. Neat MAPbI$_3$ has a bandgap of 1.53eV, which is correlated with reported optical bandgap data [1, 40, 42].

5. CONCLUSION

In summary, 2D $TBAPbBr_xI_{3-x}$ perovskite was successfully fabricated on the top of the 3D $MAPbI_3$ perovskite film. Although the $TBAPbBr_xI_{3-x}$ film has a better grain structure, the application of $TBAPbBr_xI_{3-x}$ alone in the solar cells is difficult due to the poor light absorption in the visible spectrum. However, it can be used as a separate layer on the top of the 3D $MAPbI_3$ perovskite layer and it can close pinholes in the 3D $MAPbI_3$ perovskite film.

6. RECOMMENDATIONS AND FUTURE WORK

A Detailed study on;

- The ability of shielding from moisture and degradation of the 2D perovskite capping layer on top of the 3D perovskite structure.
- 2D perovskite capping layer capacity and interference to diminish charge recombination and encourage hole transportation at the interface when it paced on top of the 3D perovskite structure.
- The solar cell fabrication with the 2D TBAPbBr$_x$I$_{3-x}$ alone and as a capping layer on top of the 3D perovskite structure.
- Optoelectronic properties including PCE in the cell structure analysis for better understanding.

REFERENCES

[1] K. P. Bhandari and R. J. Ellingson, '11 - An Overview of Hybrid Organic–Inorganic Metal Halide Perovskite Solar Cells', in *A Comprehensive Guide to Solar Energy Systems*, T. M. Letcher and V. M. Fthenakis, Eds. Academic Press, 2018, pp. 233–254.

[2] T. M. Brenner, D. A. Egger, L. Kronik, G. Hodes, and D. Cahen, 'Hybrid organic—inorganic perovskites: low-cost semiconductors with intriguing charge-transport properties', *Nature Reviews Materials*, vol. 1, no. 1, pp. 1–16, Jan. 2016, doi: 10.1038/natrevmats.2015.7.

[3] A. Kojima, K. Teshima, Y. Shirai, and T. Miyasaka, 'Organometal Halide Perovskites as Visible-Light Sensitizers for Photovoltaic Cells', *J. Am. Chem. Soc.*, vol. 131, no. 17, pp. 6050–6051, May 2009, doi: 10.1021/ja809598r.

[4] 'A decade of perovskite photovoltaics', *Nature Energy*, vol. 4, no. 1, p. 1, Jan. 2019, doi: 10.1038/s41560-018-0323-9.

[5] B. Billstrand, K. Bian, L. Alarid, and H. Fan, 'Surfactant-Assisted Synthesis of Monodisperse Methylammonium Lead Iodide Perovskite Nanocrystals', *j nanosci nanotechnol*, vol. 19, no. 1, pp. 465–469, Jan. 2019, doi: 10.1166/jnn.2019.15768.

[6] D. H. Cao, C. C. Stoumpos, O. K. Farha, J. T. Hupp, and M. G. Kanatzidis, '2D Homologous Perovskites as Light-Absorbing Materials for Solar Cell Applications', *J. Am. Chem. Soc.*, vol. 137, no. 24, pp. 7843–7850, Jun. 2015, doi: 10.1021/jacs.5b03796.

[7] W. Li, Z. Wang, F. Deschler, S. Gao, R. H. Friend, and A. K. Cheetham, 'Chemically diverse and multifunctional hybrid organic–inorganic perovskites', *Nat Rev Mater*, vol. 2, no. 3, p. 16099, Mar. 2017, doi: 10.1038/natrevmats.2016.99.

[8] G. Grancini *et al.*, 'One-Year stable perovskite solar cells by 2D/3D interface engineering', *Nature Communications*, vol. 8, p. 15684, Jun. 2017, doi: 10.1038/ncomms15684.

[9] P. C. Reshmi Varma, 'Chapter 7 - Low-Dimensional Perovskites', in *Perovskite Photovoltaics*, S. Thomas and A. Thankappan, Eds. Academic Press, 2018, pp. 197–229.

[10] 'EIA projects 28% increase in world energy use by 2040 - Today in Energy - U.S. Energy Information Administration (EIA)'. [Online]. Available: https://www.eia.gov/todayinenergy/detail.php?id=32912. [Accessed: 25-Feb-2020].

[11] D. M. Chapin, C. S. Fuller, and G. L. Pearson, 'A New Silicon p-n Junction Photocell for Converting Solar Radiation into Electrical Power: Journal of Applied Physics: Vol 25, No 5', 1954. [Online]. Available: https://aip.scitation.org/doi/10.1063/1.1721711. [Accessed: 12-Nov-2019].

[12] 'Theory of solar cells', *HiSoUR - Hi So You Are*, 26-Sep-2018. [Online]. Available: https://www.hisour.com/theory-of-solar-cells-39930/. [Accessed: 25-Feb-2020].

[13] R. M. R.M. Swanson, '(1) Approaching the 29% limit efficiency of silicon solar cells', *ResearchGate*. [Online]. Available: https://www.researchgate.net/publication/224618310_Approaching_the_29_limit_efficiency_of_silicon_solar_cells. [Accessed: 25-Feb-2020].

[14] S. Rühle, 'Tabulated values of the Shockley–Queisser limit for single junction solar cells', *Solar Energy*, vol. 130, pp. 139–147, Jun. 2016, doi: 10.1016/j.solener.2016.02.015.

[15] 'AgoraEnergiewende_Current_and_Future_Cost_of_PV_Feb2015_web.pdf'. .

[16] 'efficiency-chart.png (1200×665)'. [Online]. Available: https://www.nrel.gov/pv/assets/images/efficiency-chart.png. [Accessed: 13-Nov-2019].

[17] T. Wolfram and S. Ellialtioglu, 'Electronic and Optical Properties of d-Band Perovskites by Thomas Wolfram', *Cambridge Core*, Oct-2006. [Online]. Available: /core/books/electronic-and-optical-properties-of-dband-perovskites/2C2E18559097C1F812F76ED59A4DBCE8. [Accessed: 20-May-2019].

[18] N. F. Atta, A. Galal, and E. H. El-Ads, 'Perovskite Nanomaterials – Synthesis, Characterization, and Applications', *Perovskite Materials - Synthesis, Characterisation, Properties, and Applications*, Feb. 2016, doi: 10.5772/61280.
[19] N.-G. Park, 'Perovskite solar cells: an emerging photovoltaic technology', *Materials Today*, vol. 18, no. 2, pp. 65–72, Mar. 2015, doi: 10.1016/j.mattod.2014.07.007.
[20] C. Li, X. Lu, W. Ding, L. Feng, Y. Gao, and Z. Guo, 'Formability of ABX3 (X = F, Cl, Br, I) halide perovskites', *Acta Crystallogr., B*, vol. 64, no. Pt 6, pp. 702–707, Dec. 2008, doi: 10.1107/S0108768108032734.
[21] J. Berry *et al.*, 'Hybrid Organic-Inorganic Perovskites (HOIPs): Opportunities and Challenges', *Adv. Mater. Weinheim*, vol. 27, no. 35, pp. 5102–5112, Sep. 2015, doi: 10.1002/adma.201502294.
[22] A. K. Cheetham and C. N. R. Rao, 'There's Room in the Middle', *Science*, vol. 318, no. 5847, pp. 58–59, Oct. 2007, doi: 10.1126/science.1147231.
[23] 'Best Research-Cell Efficiencies'. National Renewable Energy Laboratory.
[24] D. B. Mitzi, 'Solution-processed inorganic semiconductors', *J. Mater. Chem.*, vol. 14, no. 15, p. 2355, 2004, doi: 10.1039/b403482a.
[25] Z. Xiao, Q. Dong, C. Bi, Y. Shao, Y. Yuan, and J. Huang, 'Solvent Annealing of Perovskite-Induced Crystal Growth for Photovoltaic-Device Efficiency Enhancement', *Adv. Mater.*, vol. 26, no. 37, pp. 6503–6509, Oct. 2014, doi: 10.1002/adma.201401685.
[26] B. R. Sutherland, 'Perovskites: Between the Grains', *Joule*, vol. 2, no. 5, pp. 820–822, May 2018, doi: 10.1016/j.joule.2018.04.024.
[27] W. Zhang *et al.*, 'Enhanced optoelectronic quality of perovskite thin films with hypophosphorous acid for planar heterojunction solar cells', *Nat Commun*, vol. 6, no. 1, p. 10030, Dec. 2015, doi: 10.1038/ncomms10030.
[28] Z. Chu *et al.*, 'Impact of grain boundaries on efficiency and stability of organic-inorganic trihalide perovskites', *Nat Commun*, vol. 8, no. 1, p. 2230, Dec. 2017, doi: 10.1038/s41467-017-02331-4.
[29] N. De Marco *et al.*, 'Guanidinium: A Route to Enhanced Carrier Lifetime and Open-Circuit Voltage in Hybrid Perovskite Solar Cells', *Nano Lett.*, vol. 16, no. 2, pp. 1009–1016, Feb. 2016, doi: 10.1021/acs.nanolett.5b04060.
[30] G. Liu *et al.*, 'Influence of the Organic Chain on the Optical Properties of Two-Dimensional Organic–Inorganic Hybrid Lead Iodide Perovskites', *ACS Appl. Electron. Mater.*, vol. 1, no. 11, pp. 2253–2259, Nov. 2019, doi: 10.1021/acsaelm.9b00466.
[31] L. Dou *et al.*, 'Atomically thin two-dimensional organic-inorganic hybrid perovskites', *Science*, vol. 349, no. 6255, pp. 1518–1521, Sep. 2015, doi: 10.1126/science.aac7660.
[32] Q. Xu, D. Yang, J. Lv, Y.-Y. Sun, and L. Zhang, 'Perovskite Solar Absorbers: Materials by Design', *Small Methods*, vol. 2, no. 5, p. 1700316, 2018, doi: 10.1002/smtd.201700316.
[33] F. Brivio, K. T. Butler, A. Walsh, and M. van Schilfgaarde, 'Relativistic quasiparticle self-consistent electronic structure of hybrid halide perovskite photovoltaic absorbers', *Phys. Rev. B*, vol. 89, no. 15, p. 155204, Apr. 2014, doi: 10.1103/PhysRevB.89.155204.
[34] Y. Han *et al.*, 'Degradation observations of encapsulated planar CH3NH3PbI3 perovskite solar cells at high temperatures and humidity', *J. Mater. Chem. A*, vol. 3, no. 15, pp. 8139–8147, Mar. 2015, doi: 10.1039/C5TA00358J.
[35] H. Zhang *et al.*, 'Improved Performance of Perovskite Light-Emitting Diodes by Dual Passivation with an Ionic Additive', *ACS Appl. Energy Mater.*, p. acsaem.9b00186, Apr. 2019, doi: 10.1021/acsaem.9b00186.
[36] I. Poli, S. Eslava, and P. Cameron, 'Tetrabutylammonium cations for moisture-resistant and semitransparent perovskite solar cells', *Journal of Materials Chemistry A*, vol. 5, no. 42, pp. 22325–22333, 2017, doi: 10.1039/C7TA06735F.

[37] S. N. Habisreutinger, T. Leijtens, G. E. Eperon, S. D. Stranks, R. J. Nicholas, and H. J. Snaith, ‘Carbon Nanotube/Polymer Composites as a Highly Stable Hole Collection Layer in Perovskite Solar Cells’, *Nano Lett.*, vol. 14, no. 10, pp. 5561–5568, Oct. 2014, doi: 10.1021/nl501982b.
[38] S. Yang, Y. Wang, P. Liu, Y.-B. Cheng, H. J. Zhao, and H. G. Yang, ‘Functionalization of perovskite thin films with moisture-tolerant molecules’, *Nat Energy*, vol. 1, no. 2, p. 15016, Feb. 2016, doi: 10.1038/nenergy.2015.16.
[39] S. Eslava *et al.*, ‘Zeolite-inspired low-k dielectrics overcoming limitations of zeolite films’, *Journal of the American Chemical Society*, vol. 130, no. 51, pp. 17528–17536, Dec. 2008, doi: 10.1021/ja8066572.
[40] K. Yao, X. Wang, F. Li, and L. Zhou, ‘Mixed perovskite based on methyl-ammonium and polymeric-ammonium for stable and reproducible solar cells’, *Chem. Commun.*, vol. 51, no. 84, pp. 15430–15433, Oct. 2015, doi: 10.1039/C5CC05879A.
[41] C. Ma *et al.*, ‘2D/3D perovskite hybrids as moisture-tolerant and efficient light absorbers for solar cells’, *Nanoscale*, vol. 8, no. 43, pp. 18309–18314, 2016, doi: 10.1039/C6NR04741F.
[42] C. Quarti, N. Marchal, and D. Beljonne, ‘Tuning the Optoelectronic Properties of Two-Dimensional Hybrid Perovskite Semiconductors with Alkyl Chain Spacers’, *J. Phys. Chem. Lett.*, vol. 9, no. 12, pp. 3416–3424, Jun. 2018, doi: 10.1021/acs.jpclett.8b01309.
[43] K. Sun, J. Chang, F. H. Isikgor, P. Li, and J. Ouyang, ‘Efficiency enhancement of planar perovskite solar cells by adding zwitterion/LiF double interlayers for electron collection’, *Nanoscale*, vol. 7, no. 3, pp. 896–900, 2015, doi: 10.1039/C4NR05975A.

APPENDIX I

SEM Images of $MAPbI_3$ at Different Magnification

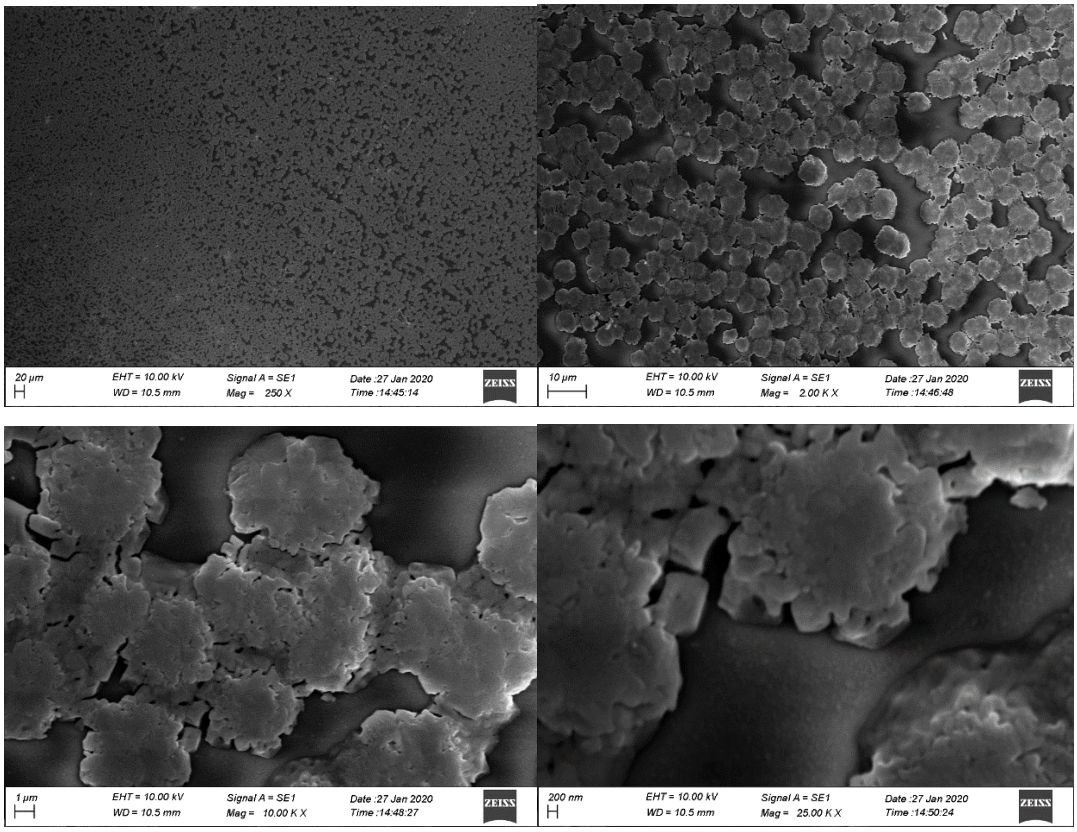

Figure 13-SEM images of $MAPbI_3$ at different magnification

APPENDIX II

X-ray diffraction (XRD) is a powerful non-destructive technique for characterizing crystalline materials. It provides information on structures, phases, preferred crystal orientations, and other structural parameters, such as average grain size, crystallinity, strain, and crystal defects.

X-ray diffraction is based on constructive interference of monochromatic X-rays and a crystalline sample. These X-rays are generated by a cathode ray tube, filtered to produce monochromatic radiation, collimated to concentrate, and directed toward the sample Figure 14.

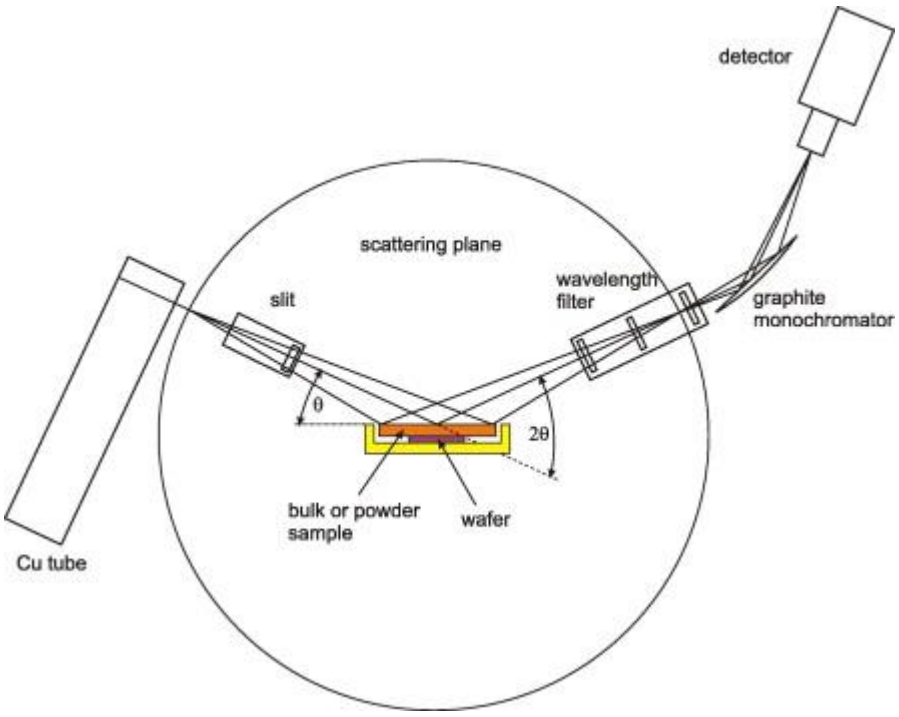

Figure 14- Schematic representation of XRD

The interaction of the incident rays with the sample produces constructive interference (and a diffracted ray) when conditions satisfy Bragg's law:

$$n\lambda = 2d\sin\theta \quad (6)$$

where n is an integer, λ is the wavelength of the X-rays, d is the interplanar spacing generating the diffraction, and θ is the diffraction angle.

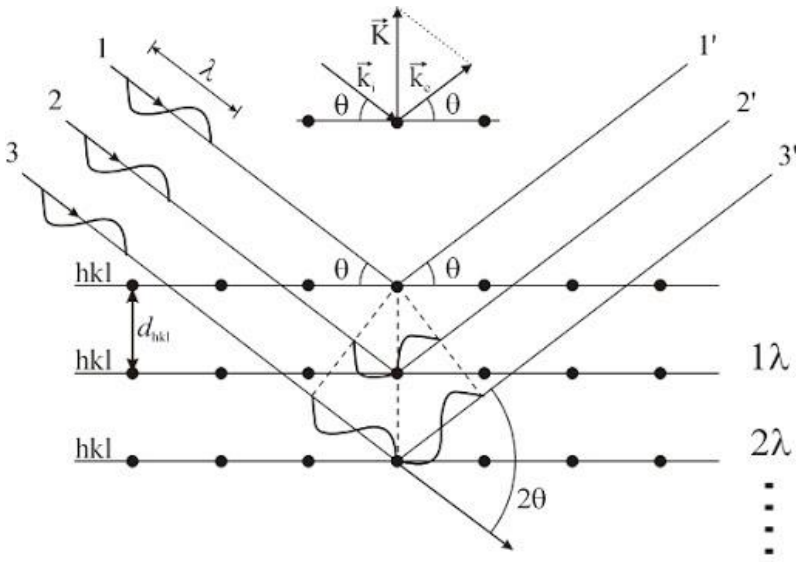

Figure 15- Principle of XRD

The peak intensities are determined by the placing of atoms within the lattice. Therefore, the X-ray diffraction pattern is the fingerprint of periodic atomic arrangements in a given material.

The Bragg equation, which describes diffraction of a three-dimensional crystal, fails in two-dimensional (2D) cases. Complete integration of diffraction signals from a continuum instead of discrete directions in the Bragg equation is therefore essential for proper data analysis of 2D materials.

Literature mentioned that 2D perovskite materials have consistent peaks at lower angles ($2\theta < 10°$) [6,8, 36,41, 43]. Considering the above fact, it is concluded that distinguishable diffraction peak at 7.59° in $TBAPbBr_xI_{3-x}$ perovskite XRD spectrum can identify as the characteristic peak that determines the formation 2D perovskite structure.